

## 82. Photophysical Properties and Photochemical Behaviour of Ruthenium(II) Complexes Containing the 2,2'-Bipyridine and 4,4'-Diphenyl-2,2'-Bipyridine Ligands

by Luisa De Cola and Francesco Barigelletti\*

Istituto FRAE-CNR, v. dei Castagnoli 1, I-40126 Bologna

and Michael J. Cook

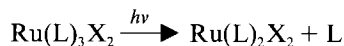
School of Chemical Sciences, University of East Anglia, Norwich NR4 7TJ, UK

(11. III. 88)

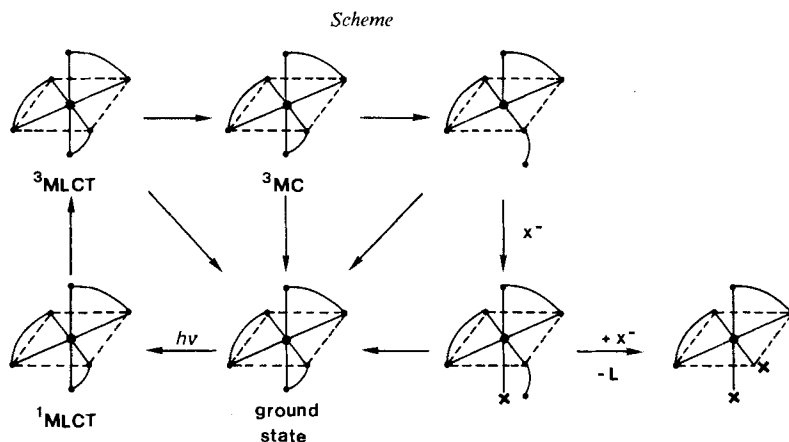
The temperature dependence of the emission lifetime of the series of complexes  $\text{Ru}(\text{bpy})_n(4,4'\text{-dph})_3^{2+}$  ( $\text{bpy} = 2,2'$ -bipyridine,  $4,4'\text{-dph} = 4,4'$ -diphenyl-2,2'-bipyridine) has been studied in propionitrile/butyronitrile (4:5 v/v) solutions in the range 90–293 K. The obtained photophysical parameters show that the energy separation between the metal-to-ligand charge transfer ( $^3\text{MLCT}$ ) emitting level and the photoreactive metal-centered ( $^3\text{MC}$ ) level changes across the series ( $\Delta E = 3960, 4100, 4300,$  and  $4700 \text{ cm}^{-1}$  for  $\text{Ru}(\text{bpy})_3^{2+}$ ,  $\text{Ru}(\text{bpy})_2(4,4'\text{-dph})_2^{2+}$ ,  $\text{Ru}(\text{bpy})(4,4'\text{-dph})_3^{2+}$ , and  $\text{Ru}(4,4'\text{-dph})_3^{2+}$ , respectively, where  $\Delta E$  is the energy separation between the minimum of the  $^3\text{MLCT}$  potential curve and  $^3\text{MLCT} - ^3\text{MC}$  crossing point). Comparison between spectral and electrochemical data indicates that the changes in  $\Delta E$  are due to stabilization of the MLCT levels in complexes containing  $4,4'\text{-dph}$  with respect to  $\text{Ru}(\text{bpy})_3^{2+}$ . The photochemical data for the same complexes (as  $\text{I}^-$  salts) have been obtained in  $\text{CH}_2\text{Cl}_2$  in the presence of  $0.01 \text{ M Cl}^-$  upon irradiation at 462 nm. The complexes containing  $4,4'\text{-dph}$  are more photostable than  $\text{Ru}(\text{bpy})_3^{2+}$ . Comparison between the data for thermal population of the  $^3\text{MC}$  photoreactive state and those for photochemistry indicates that the overall photochemical process is governed by *i*) thermal redistribution between the emitting and photoreactive excited states, and *ii*) mechanistic factors, likely related to the size of the detaching ligand.

**Introduction.** – In recent years, the potential use of Ru-polypyridine complexes as sensitizers in photoinduced redox processes has led to an impressive growth of research activity concerned with electrochemical, spectroscopic, and photophysical properties of hundreds of complexes [1–10]. The large number of investigated complexes has led to well-established correlations between electrochemical and spectroscopic data [10–14] and, as a consequence, to the feasibility of ‘tuning’ procedures, *i.e.* selection of complexes to fit specific spectroscopic and/or electrochemical requirements.

The practical use of Ru-polypyridine complexes is, however, restricted by their photochemical instability [1][6][9]. In fact, it is known that in solvents which favour ion pairs (*e.g.*  $\text{CH}_2\text{Cl}_2$ , dielectric constant  $\epsilon = 9.1$ ) photoanation takes place, *viz.*



For example, for  $\text{Ru}(\text{bpy})_3\text{Cl}_2$  in aerated  $\text{CH}_2\text{Cl}_2$ , the photoanation quantum yield  $\Phi_p = 0.062$  [15], while for the same complex in  $\text{H}_2\text{O}$  ( $\epsilon = 80.2$ )  $\Phi_p < 10^{-4}$  [16a]. Photo-substitution has been reported to occur according to a two-steps mechanism [15], whose critical steps are affected by the dielectric properties of the solvent and by the anion size



[15]. Reference to the *Scheme* shows that also the size of L could lead to detectable effects concerned with its displacements. On the other hand, photophysical studies (mainly temperature dependence of emission properties [3][9][10a][15–20]) have shown that the photochemical lability of Ru-polypyridine complexes is related to the thermal accessibility, during the lifetime of the emitting metal-to-ligand charge transfer ( $^3\text{MLCT}$ ) excited state, of a higher-energy metal-centered excited state ( $^3\text{MC}$ ), a so-called doorway to photochemistry.

Synthetic control of the energy separation between  $^3\text{MLCT}$  and  $^3\text{MC}$  levels can be proposed as a key to control photochemistry in mixed-ligand complexes [19][21][22]. Stabilization of the  $^3\text{MLCT}$  state can be achieved by employing ligands having low-lying accepting orbitals, for instance ligands with extended  $\pi$  conjugation [23]. However, in this case the increased size of the ligands may result in a certain amount of interligand hindrance, leading to decreased ligand strength and stabilization of the  $^3\text{MC}$  state, and consequently to more efficient photochemistry.

Consideration of the molecular structure of 4,4'-dpb indicates that no increased interligand hindrance is expected in complexes containing it with respect to the case of  $\text{Ru}(\text{bpy})_3^{2+}$ . We have, therefore, investigated the  $\text{Ru}(\text{bpy})_n(4,4'\text{-dpb})_{3-n}^{2+}$  series in an attempt to provide further insight into the correlations between spectroscopy, electrochemistry, photophysics, and photochemistry in Ru-polypyridine complexes.

**Experimental.** – The complexes were prepared as described in [7a]. The employed solvents were of the best grade commercially available.

Absorption spectra were recorded on a *Kontron Uvikon 860* spectrophotometer and uncorrected emission spectra on a *Perkin-Elmer MPF-44B* spectrofluorimeter equipped with a *Hamamatsu R928* phototube.

The experiments on temperature dependence of emission properties were carried out in propionitrile/butyronitrile solns. (4:5 v/v). The samples ( $10^{-4}$ – $10^{-5}$  M) were sealed under vacuum in 1-cm quartz cells after repeated freeze-pump-thaw cycles. The cells were placed inside a modified *C600 Thor* cryostat, and the temp. control ( $\pm 2\text{K}$ ) was achieved by a *3050 Thor* temp. controller.

The emission lifetimes were measured using a modified *Applied Photophysics* single-photon equipment. Single exponential analysis was applied throughout employing non-linear least-squares iterative reconvolution programs [24]. The uncertainty in lifetime measurements is  $\leq 7\%$ . The temp. dependence of the lifetime was analyzed using standard iterative programs. Data treatment was carried out with a *Digital PDP 11/23* microcomputer.

Light excitation in the photochemical experiments was performed with a W lamp and using a 462-nm interference filter. The number of Einsteins incident on the reaction cell was determined by means of the *Aber-*

chrome 540 chemical actinometer [25]. The photochemical quantum yields for reactant disappearance,  $\Phi_p$ , were calculated monitoring the decrease in intensity of the lowest-energy absorption band of the starting complex and following standard procedures [26]. Isosbestic points for the spectra of the starting complexes and photoproducts were always observed. Photolysis experiments were performed in  $\text{CH}_2\text{Cl}_2$  and in  $\text{CH}_3\text{CN}$  in the presence of 0.01M benzyl(triethyl)ammonium chloride, but only data obtained in  $\text{CH}_2\text{Cl}_2$  are reported here. The uncertainty in  $\Phi_p$  is estimated to be  $\leq 10\%$ . The products of photolysis of the mixed-ligand complexes have been identified on the basis of their absorption spectra for bpy and 4,4'-dpb ligands.

**Results.** – Table 1 reports the absorption and emission band maxima and emission lifetimes at room temperature and at 90 K for the  $\text{Ru}(\text{bpy})_n(4,4'\text{-dpb})_{3-n}^{2+}$  complexes in the indicated solvents. Spectral data at room temperature were previously reported in  $\text{CH}_3\text{CN}$  [11] and  $\text{EtOH/MeOH}$  (4:1 v/v) [7a], and comparison of the results indicates only a slight solvent effect. The first oxidation and reduction potentials for the complexes [11] are also reported in Table 1.

Table 1. Photophysical and Electrochemical Data of  $\text{Ru}(\text{bpy})_n(4,4'\text{-dpb})_{3-n}^{2+}$  Complexes in Propionitrile/Butyronitrile Solution unless Otherwise Specified

	Room temperature					90 K	
	$\lambda_{\text{abs}} (\epsilon)^a$ [nm]	$\lambda_{\text{em}}$ [nm]	$\tau_{\text{em}}$ [ $\mu\text{s}$ ]	$E_{1/2}(\text{ox})^b$ [V]	$E_{1/2}(\text{red})^b$ [V]	$\lambda_{\text{em}}$ [nm]	$\tau_{\text{em}}$ [ $\mu\text{s}$ ]
$\text{Ru}(\text{bpy})_3^{2+}$	451 (14300)	617	1.11	1.23	-1.35	575	4.74
$\text{Ru}(\text{bpy})_2(4,4'\text{-dpb})^{2+}$	459 (17900)	628	1.35	1.23	-1.31	600	4.0
$\text{Ru}(\text{bpy})(4,4'\text{-dpb})_2^{2+}$	467 (14700)	631	1.64	1.20	-1.30	616	3.35
$\text{Ru}(4,4'\text{-dpb})_3^{2+}$	477 (28000)	638	1.68	1.19	-1.27	606	3.6
bpy					-2.22		
4,4'-dpb					-2.06 <sup>c)</sup>		

<sup>a)</sup> In  $\text{CH}_3\text{CN}$ .

<sup>b)</sup> In  $\text{CH}_3\text{CN}$ , vs. SCCE [11], unless otherwise stated.

<sup>c)</sup> This work, in  $\text{CH}_3\text{CN}$ , vs. SCCE.

The temperature dependence of the emission lifetimes in propionitrile/butyronitrile solution is shown in Fig. 1. For all the complexes, a similar behaviour is registered. Starting from 90 K and increasing the temperature, the lifetime markedly shortens in the interval 100–150 K (the glass-to-fluid transition region of the solvent [23]). Further heating causes a smooth decrease of the lifetime until, above a well determined temperature, the lifetime decrease becomes steep again. Fig. 1 indicates that this final downbending starts at higher and higher temperature going from  $\text{Ru}(\text{bpy})_3^{2+}$  to  $\text{Ru}(4,4'\text{-dpb})_3^{2+}$ . Eqn. 1 was employed to fit the  $\tau$  vs.  $T$  data [16b][23]

$$\tau = (k'_0 + k_1 + k_2)^{-1} \quad (1)$$

where  $k'_0 = k_0 + B$ ,  $k_1 = A_1 \cdot \exp(-\Delta E_1/RT)$  and  $k_2 = A_2 \cdot \exp(-\Delta E_2/RT)$ .

In Eqn. 1,  $k_0$  is a low-temperature (90 K) limiting rate including both radiative and non-radiative contributions,  $B$  is a rate corresponding to the increase of radiationless contributions taking place in the glass-to-fluid transition region of the solvent [23],  $A_1$  and  $\Delta E_1$  as well as  $A_2$  and  $\Delta E_2$  are preexponential factors and energy barriers, respectively, for Arrhenius-like processes. The kinetic parameters extracted from the fitting procedure are reported in Table 2. Parameters concerning the glass-to-fluid transition region of the solvent [23][27][28] will be presented and discussed elsewhere [29].

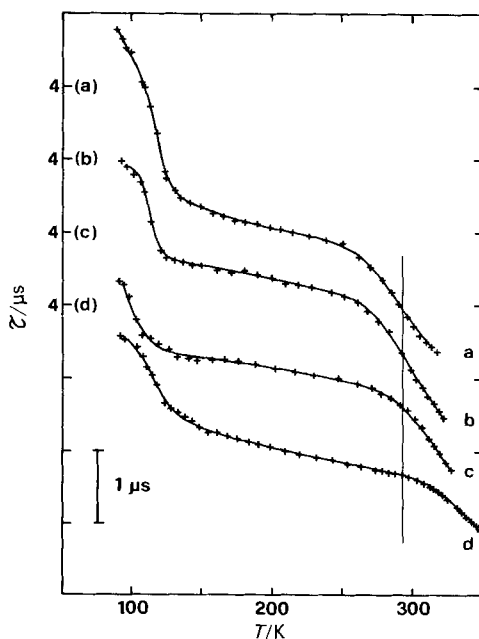


Fig. 1. Temperature dependence of the emission lifetime in propionitrile/butyronitrile solution:  $\text{Ru}(\text{bpy})_3^{2+}$  (a),  $\text{Ru}(\text{bpy})_2(4,4'\text{-dpb})^{2+}$  (b),  $\text{Ru}(\text{bpy})(4,4'\text{-dpb})_2^{2+}$  (c), and  $\text{Ru}(4,4'\text{-dpb})_3^{2+}$  (d). The vertical line marks the room temperature.

Table 2. Kinetic Parameters Extracted from the Fitting of Eqn. 1 to the Experimental Results of Fig. 1

	$k_0$ [ $\text{s}^{-1}$ ]	$A_1$ [ $\text{s}^{-1}$ ]	$\Delta E_1$ [ $\text{cm}^{-1}$ ]	$A_2$ [ $\text{s}^{-1}$ ]	$\Delta E_2$ [ $\text{cm}^{-1}$ ]
$\text{Ru}(\text{bpy})_3^{2+}$	$2.3 \cdot 10^5$	$5.6 \cdot 10^5$	90	$1.4 \cdot 10^{14}$	3960
$\text{Ru}(\text{bpy})_2(4,4'\text{-dpb})^{2+}$	$3.7 \cdot 10^5$	$6.7 \cdot 10^5$	350	$1.5 \cdot 10^{14}$	4100
$\text{Ru}(\text{bpy})(4,4'\text{-dpb})_2^{2+}$	$4.3 \cdot 10^5$	$1.2 \cdot 10^6$	480	$1.2 \cdot 10^{14}$	4300
$\text{Ru}(4,4'\text{-dpb})_3^{2+}$	$3.8 \cdot 10^5$	$8.7 \cdot 10^5$	300	$1.0 \cdot 10^{14}$	4700

Table 3. Photolysis in 0.01 M  $\text{Cl}^-/\text{CH}_2\text{Cl}_2$

	$\Phi_p^a$	$\Phi_d^b$	$\Phi_{dp}^c$
$\text{Ru}(\text{bpy})_3\text{I}_2$	$9.2 \cdot 10^{-3}$	0.126	0.073
$\text{Ru}(\text{bpy})_2(4,4'\text{-dpb})\text{I}_2$	$1.7 \cdot 10^{-3}$	0.074	0.023
$\text{Ru}(\text{bpy})(4,4'\text{-dpb})_2\text{I}_2$	$2.4 \cdot 10^{-4}$	0.023	0.01
$\text{Ru}(4,4'\text{-dpb})_3^{2+}$		0.003	

<sup>a</sup>) Photochemical quantum yield for reactant disappearance.

<sup>b</sup>) Efficiency for thermal population of the  $^3\text{MC}$  state, calculated taking into account oxygen quenching:  
 $\Phi_d = \Phi_{isc} \cdot k_2 \cdot \tau_q$ .

<sup>c</sup>) Intrinsic photochemical efficiency of the  $^3\text{MC}$  state once thermally populated.

**Discussion.** – The spectral data in Table 1 show that sequential substitution of 4,4'-dpb for bpy leads to gradual shift of the lowest-energy absorption maximum. As is well known, this band corresponds to the transition from the ground state to the lowest-energy  $^1\text{MLCT}$  excited state [3]. According to a simple orbital picture, this transition is

viewed as electron promotion from a metal d orbital to the lowest unoccupied ligand orbital. If one assumes a localized description [4], the accepting orbital is centered on a single ligand. Comparison of the reduction potentials for the free ligands (*Table 1*) indicates that the lowest unoccupied orbital (LUMO) of 4,4'-dpb is lower in energy by *ca.* 0.16 eV than that of bpy. On this basis, for the mixed-ligand complexes examined, one expects a major involvement of 4,4'-dpb in the one-electron reduction as well as in the Ru→ligand lowest-energy optical transition. However, the energy separation between the LUMO's of the two ligands is not large (0.16 eV), and, therefore, the single configurational excited state description is unlikely to be strictly valid. Plotting the absorption energies *vs.* electrochemical energies,  $\Delta E_{1/2} = e[E_{1/2}(\text{ox}) - E_{1/2}(\text{red})]$ , where *e* is the electron charge, results in a fairly good linear relation (*Fig. 2*) according to *Eqn. 2* [10–14]

$$h\nu_{\text{abs}}^{\text{max}} = \Delta E_{1/2} + A \quad (2)$$

One concludes that electron removal (from the metal d orbital) and promotion (to LUMO) take place in a similar way either in redox or in optical (absorption) processes<sup>1</sup>).

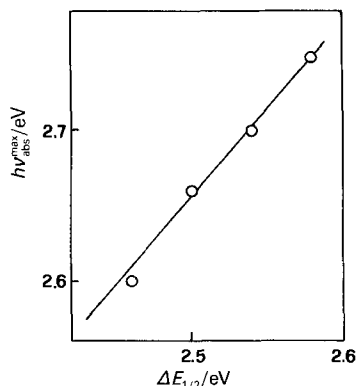


Fig. 2. Correlation between the redox energy,  $\Delta E_{1/2}$ , and the energy of the <sup>1</sup>MLCT absorption maximum according to *Eqn. 2*. Linear regression parameters: slope = 1.07, intercept = -0.02 eV, *r* = 0.998.

Closer examination of the electrochemical data (*Table 1*) indicates that on going from Ru(bpy)<sub>3</sub><sup>2+</sup> to Ru(4,4'-dpb)<sub>3</sub><sup>2+</sup>,  $E_{1/2}(\text{ox})$  decreases by 0.04 eV and  $E_{1/2}(\text{red})$  increases by 0.08 eV. For related Ru complexes, it has been demonstrated that the  $E_{1/2}(\text{ox})$  values depend upon the ligand basicity, an increase by *ca.* 2 p*K<sub>a</sub>* units corresponding to a decrease of  $E_{1/2}(\text{ox})$  by *ca.* 0.15 eV [7c]. Consideration of the *Hammett*  $\sigma$  constant for the Ph group [7c] also suggests that the two ligands have close p*K<sub>a</sub>* values. One concludes, therefore, that bpy and 4,4'-dpb ligands should practically exhibit the same ligand basicity. In the absence of steric factors, the basicity of the ligand is the main factor modulating the field strength and the <sup>3</sup>MC (ligand field) states are expected to be nearly isoenergetic. On the other hand, the spectroscopic data (*Table 1*) indicate that the MLCT levels move to lower energies going from Ru(bpy)<sub>3</sub><sup>2+</sup> to Ru(4,4'-dpb)<sub>3</sub><sup>2+</sup>. The schematic

<sup>1</sup>) In comparing electrochemical and spectroscopic data, one should use 0–0 energies. We assume, however, that for the examined complexes the difference between the spectral maximum and related 0–0 energy is a constant quantity.

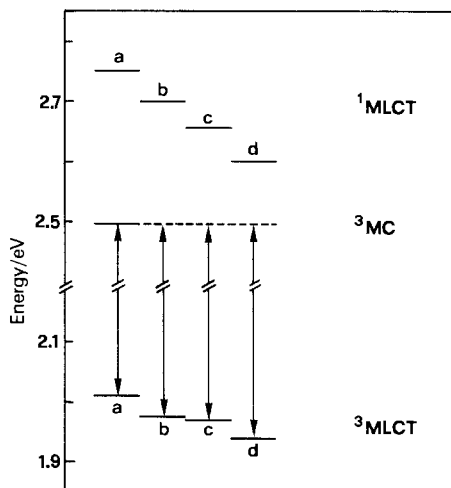


Fig. 3. Energy levels corresponding to the room-temperature spectral maxima for  $\text{Ru}(\text{bpy})_3^{2+}$  (a),  $\text{Ru}(\text{bpy})_2(4,4'\text{-dpp})^{2+}$  (b),  $\text{Ru}(\text{bpy})(4,4'\text{-dpp})^{2+}$  (c), and  $\text{Ru}(4,4'\text{-dpp})_3$  (d). See text for further details.

diagram in Fig. 3 shows the energy position of  $^1\text{MLCT}$  and  $^3\text{MLCT}$  energy levels as determined from spectral maxima. The energy separation between the  $^3\text{MLCT}$  emitting state and the  $^3\text{MC}$  state is expected to increase regularly across the series. In Fig. 3, the reported energy position of the  $^3\text{MC}$  levels is that for  $\text{Ru}(\text{bpy})_3^{2+}$  (see below).

The kinetic parameters collected in Table 2 can be discussed as follows. Population of  $^1\text{MLCT}$  excited state by light absorption leads to the  $^3\text{MLCT}$  emitting state. As pointed out by many authors for  $\text{Ru}(\text{bpy})_3^{2+}$ , [3][9][10a][15–20] at  $T < 250$  K the emission lifetime is affected by: *i*) temperature-independent paths ( $k_0$  at 90 K in our case), *ii*) processes occurring in the glass-to-fluid transition interval ( $B$ ) [23][27][28], and *iii*) thermal redistribution within a cluster of closely spaced  $^3\text{MLCT}$  states ( $k_1$ ), while for  $T > 250$  K, thermal activation to the  $^3\text{MC}$  state takes place ( $k_2$ ). The close similarity of  $\tau$  vs.  $T$  curves for the examined complexes (Fig. 1) and the temperature dependence of the emission intensities (not reported) suggest that the same processes affect  $\tau$  in our series even if, passing from  $\text{Ru}(\text{bpy})_3^{2+}$  to  $\text{Ru}(4,4'\text{-dpp})_3^{2+}$ , there is a reduced contribution to the deactivation of the excited state of the process associated with  $k_2$  ( $T > 250$  K).

The meaning of the experimental quantities  $A_2$  and  $\Delta E_2$  (Table 2) has been discussed with reference to three limiting cases [15][27a], depending on the balance among  $k_a$ ,  $k_b$ , and  $k_c$  of Fig. 4. For  $\text{Ru}(\text{bpy})_3^{2+}$ , it has been assumed that  $k_c \gg k_b$  and that  $A_2$  ( $\sim 10^{14} \text{ s}^{-1}$ ) and  $\Delta E_2$  ( $3960 \text{ cm}^{-1}$ ) correspond to  $A_a$  and  $\Delta E_a$ , respectively, where  $\Delta E_a$  is the energy barrier taken from the minimum of the potential curve for the  $^3\text{MLCT}$  and the crossing point between the  $^3\text{MLCT}$  and  $^3\text{MC}$  curves. In this case,  $k_2$  represents the rate for thermal population of  $^3\text{MC}$  state and

$$\Phi_d = \Phi_{\text{isc}} \cdot k_2 \tau \quad (3)$$

is the relevant quantum yield. As seen above, going from  $\text{Ru}(\text{bpy})_3^{2+}$  to  $\text{Ru}(4,4'\text{-dpp})_3^{2+}$ , the stabilization of the  $^3\text{MLCT}$  level as determined from the room-temperature emission maxima is  $560 \text{ cm}^{-1}$ , and that for  $^1\text{MLCT}$  as determined from the lowest-energy absorp-

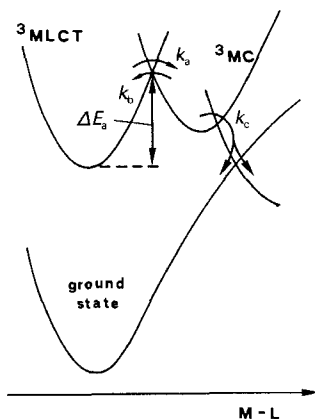


Fig. 4. Schematic representation of the potential energy curves for  ${}^3\text{MLCT}$  and  ${}^3\text{MC}$  states. For  $\text{Ru}(\text{bpy})_3^{2+}$ ,  $k_c \gg k_b$  and the experimental  $k_2 = k_a = A_a \cdot \exp(-\Delta E_a/RT)$  [16][28].

tion maxima is  $1200 \text{ cm}^{-1}$ . From the photophysical measurements and following the same order, the increase in  $\Delta E_2$  is  $740 \text{ cm}^{-1}$ , while  $A_2$  is  $\sim 10^{14} \text{ s}^{-1}$  in all cases (Table 2). These results suggest that the same kinetic scheme can be assumed throughout the series, and that the change in  $\Delta E_2$  is ascribable to the change in energy separation between the  ${}^3\text{MLCT}$  and  ${}^3\text{MC}$  level consequent to  ${}^3\text{MLCT}$  state stabilization. As a consequence,  $\Phi_d$  can be calculated according to Eqn. 3, if unit  $\Phi_{\text{isc}}$  is taken in each case [30].

Table 3 reports the quantum yield for photochemistry,  $\Phi_p$ , obtained in  $\text{O}_2$ -equilibrated  $\text{CH}_2\text{Cl}_2$  with  $\text{Cl}^-$  added (0.01M). Also reported is  $\Phi_d$ , calculated as described above from the obtained kinetic parameters (Table 2) and taking into account the quenching of  ${}^3\text{MLCT}$  emission by  $\text{O}_2$ . The quenching rate has been obtained by lifetime measurements in  $\text{O}_2$ -free and  $\text{O}_2$ -equilibrated solutions,  $k_q = (1/\tau_q) - (1/\tau)$ . The relationship between  $\Phi_p$  and  $\Phi_d$  is illustrated in Fig. 5. Increased thermal population of  ${}^3\text{MC}$  leads to increased photochemistry, even if no linear relationship is found, as expected if thermal accessibility

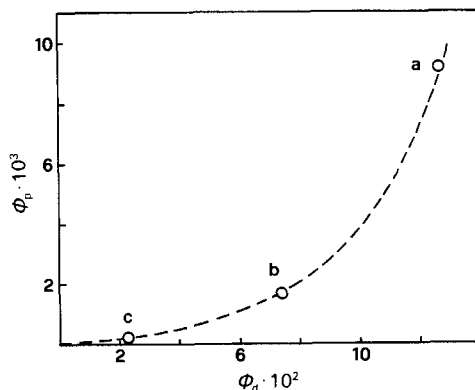


Fig. 5. Relation between thermal population ( $\Phi_d$ ) of the  ${}^3\text{MC}$  state and photochemical behaviour ( $\Phi_p$ ) in 0.01M  $\text{Cl}^-/\text{CH}_2\text{Cl}_2$ :  $\text{Ru}(\text{bpy})_3^{2+}$  (a),  $\text{Ru}(\text{bpy})_2(4,4'\text{-dpb})^{2+}$  (b), and  $\text{Ru}(\text{bpy})(4,4'\text{-dpb})_2^{2+}$  (c)

of the  $^3\text{MC}$  state were the only factor governing the photochemistry. *Table 3* also reports the intrinsic photochemical quantum yield of the  $^3\text{MC}$  state,  $\Phi_{\text{dp}}$ , obtained from *Eqn. 4* [15]

$$\Phi_{\text{p}} = \Phi_{\text{isc}} \cdot \Phi_{\text{d}} \cdot \Phi_{\text{dp}} \quad (4)$$

As one sees,  $\Phi_{\text{dp}}$  reveals a rough dependence on the number of bpy ligands of the complex, being highest in  $\text{Ru}(\text{bpy})_3^+$ . This result suggests that photochemistry takes place by preferential detachment of bpy in the mixed ligand complexes (see the *Scheme*). To check the point, the products of photolysis of the two mixed-ligand complexes have been examined. Comparison of the absorption spectra of bpy, 4,4'-dipb, and photolysis products (as extracted in heptane) confirm the above conclusion. This indicates that mechanistic factors, possibly related to the size of the ligands [31], can play an important role in the photochemistry of Ru-polypyridine complexes.

Thanks are due to Prof. V. Balzani, Dr. A. Juris, and Prof. A. J. Thomson for helpful discussions. Work done under *Programma Strategico Dinamica Molecolare* of CNR.

#### REFERENCES

- [1] K. Kalyanasundaram, *Coord. Chem. Rev.* **1982**, *46*, 159.
- [2] K. Kalyanasundaram, *J. Phys. Chem.* **1986**, *90*, 2285.
- [3] R. J. Watts, *J. Chem. Educ.* **1983**, *60*, 834.
- [4] M. K. De Armond, C. M. Carlin, *Coord. Chem. Rev.* **1981**, *36*, 325.
- [5] V. Balzani, A. Juris, F. Barigelletti, P. Belsler, A. von Zelewsky, *Riken Q.* **1984**, *78*, 78.
- [6] E. A. Seddon, K. R. Seddon, 'The Chemistry of Ruthenium', Elsevier, Amsterdam, 1984, Chapt. 15.
- [7] a) M. J. Cook, A. P. Lewis, G. S. G. McAuliff, V. Skarda, A. J. Thomson, J. L. Gasper, D. J. Robbins, *J. Chem. Soc., Perkin Trans. 2* **1984**, 1293; b) *ibid.* **1984**, 1303; c) V. Skarda, M. J. Cook, A. P. Lewis, G. S. G. McAuliff, A. J. Thomson, D. J. Robbins, *ibid.* **1984**, 1309.
- [8] G. J. Kavarnos, N. J. Turro, *Chem. Rev.* **1986**, *86*, 401.
- [9] T. J. Meyer, *Pure Appl. Chem.* **1986**, *58*, 1193.
- [10] a) A. Juris, V. Balzani, F. Barigelletti, S. Campagna, P. Belsler, A. von Zelewsky, *Coord. Chem. Rev.*, **1988**, *84*, 85; b) F. Barigelletti, A. Juris, V. Balzani, P. Belsler, A. von Zelewsky, *Inorg. Chem.* **1987**, *26*, 4116.
- [11] Y. Ohsawa, K. W. Hanck, M. K. De Armond, *J. Electroanal. Chem.* **1984**, *175*, 229.
- [12] E. S. Dodsworth, A. B. P. Lever, *Chem. Phys. Lett.* **1986**, *124*, 152 and ref. cit. therein.
- [13] a) J. C. Curtis, B. P. Sullivan, T. J. Meyer, *Inorg. Chem.* **1983**, *22*, 224; b) D. P. Rillema, G. Allen, T. J. Meyer, D. Conrad, *Inorg. Chem.* **1983**, *22*, 1617.
- [14] Y. Kawanishi, N. Kitamura, Y. Kim, S. Tazuke, *Riken, Q.* **1984**, *78*, 212.
- [15] B. Durham, J. V. Caspar, J. K. Nagle, T. J. Meyer, *J. Am. Chem. Soc.* **1982**, *104*, 4803.
- [16] a) J. Van Houten, R. J. Watts, *Inorg. Chem.* **1978**, *12*, 3381; b) J. Van Houten, R. J. Watts, *J. Am. Chem. Soc.* **1976**, *98*, 4853; c) F. E. Lytle, D. M. Hercules, *ibid.* **1969**, *91*, 253.
- [17] G. A. Crosby, *Acc. Chem. Res.* **1975**, *8*, 231.
- [18] T. J. Kemp, *Progr. React. Kinet.* **1980**, *10*, 301.
- [19] G. H. Allen, R. P. White, D. P. Rillema, T. J. Meyer, *J. Am. Chem. Soc.* **1984**, *106*, 2613.
- [20] a) W. M. Wacholtz, R. A. Auerbach, R. H. Schmehl, M. Ollino, W. R. Cherry, *Inorg. Chem.* **1985**, *24*, 1758; b) M. Ollino, W. R. Cherry, *ibid.* **1985**, *24*, 1417; c) W. F. Wacholz, R. A. Auerbach, R. H. Schmehl, *ibid.* **1986**, *25*, 227.
- [21] a) J. V. Caspar, T. J. Meyer, *Inorg. Chem.* **1983**, *22*, 2444; b) E. M. Kober, J. R. Marshall, W. J. Dressig, B. P. Sullivan, J. V. Caspar, T. J. Meyer, *ibid.* **1985**, *24*, 2755.
- [22] L. J. Henderson, W. R. Cherry, *J. Photochem.* **1985**, *28*, 143.



- [23] F. Barigelletti, A. Juris, V. Balzani, P. Belser, A. von Zelewsky, *Inorg. Chem.* **1983**, *22*, 3335.
- [24] P. R. Bevington, 'Data Reduction and Error Analysis for Physical Sciences', McGraw-Hill, New York, 1969.
- [25] H. G. Heller, J. R. Langan, *J. Chem. Soc., Perkin Trans. 2* **1981**, 341.
- [26] V. Balzani, V. Carassiti, 'Photochemistry of Coordination Compounds', Academic Press, New York, 1970.
- [27] a) F. Barigelletti, A. Juris, V. Balzani, P. Belser, A. von Zelewsky, *J. Phys. Chem.* **1987**, *91*, 1095; b) F. Barigelletti, P. Belser, A. von Zelewsky, A. Juris, V. Balzani, *ibid.* **1985**, *89*, 3680; c) F. Barigelletti, A. Juris, V. Balzani, P. Belser, A. von Zelewsky, *ibid.* **1986**, *90*, 5190.
- [28] a) J. Ferguson, E. R. Krausz, M. Maeder, *J. Phys. Chem.* **1985**, *89*, 1852; b) S. J. Milder, J. S. Gold, D. S. Kliger, *ibid.* **1986**, *90*, 548; c) J. Ferguson, E. Krausz, *Chem. Phys. Lett.* **1986**, *127*, 551; d) E. Danielson, R. S. Lumpkin, T. J. Meyer, *J. Phys. Chem.* **1987**, *91*, 1305; e) H. B. Kim, N. Kitamura, S. Tazuke, *Chem. Phys. Lett.* **1988**, *143*, 77; f) N. Kitamura, H.-B. Kim, Y. Kawanishi, R. Obata, S. Tazuke, *J. Phys. Chem.* **1986**, 1488.
- [29] L. De Cola, F. Barigelletti, unpublished results.
- [30] F. Bolletta, A. Juris, M. Maestri, D. Sandrini, *Inorg. Chim. Acta* **1980**, *44*, L175.
- [31] L. J. Henderson, M. Ollino, U. K. Gupta, G. R. Newcome, W. R. Cherry, *J. Photochem.* **1985**, *31*, 199.